



© 2021 by the author(s). This is an open access article licensed under the Creative Commons Attribution-NonCommercial-NoDerivs License (<http://creativecommons.org/licenses/by-nc-nd/4.0/>).



pages: 1 - 18

## ANALYSIS OF AERODYNAMIC PHENOMENA IN SELECTED QUARTER OF BUILDING DEVELOPMENT IN WARSAW DOWNTOWN WITH REFERENCE TO AIR POLLUTION

Agnieszka Chudzińska\*, Marta Poćwierz\*\* and Maciej Pisula\*\*

\* Department of Contemporary Architecture, Interior Design and Industrial Forms, Faculty of Architecture Warsaw University of Technology, Koszykowa 55 00-659 Warszawa,  
E-mail: [agnieszka.chudzinska@pw.edu.pl](mailto:agnieszka.chudzinska@pw.edu.pl), ORCID: 0000-0001-9765-4825

\*\* Faculty of Power and Aeronautical Engineering, Institute of Aeronautics and Applied Mechanics, Warsaw University of Technology, Nowowiejska 24, 00-665 Warsaw, Poland,  
E-mail: [mpocwie@meil.pw.edu.pl](mailto:mpocwie@meil.pw.edu.pl), ORCID: 0000-0003-0941-3840  
E-mail: [mpisula@gmail.com](mailto:mpisula@gmail.com), ORCID: 0000-0003-0618-3349

DOI: 10.24427/aea-2021-vol13-no3-01

### Abstract

Air pollution, both gaseous and in the form of dust, is a problem that affects numerous densely built-up areas of modern cities. Based on this assumption, the authors of the following paper have examined an exemplary part of urban space with various building developments located in Warsaw downtown. Both experimental and numerical studies were conducted for the two prevailing wind directions observed in this area, that is the west wind and the south-west wind.

Experimental research was conducted with the application of two known laboratory techniques, i.e., the oil visualization method and the sand erosion technique. The studies were conducted in an open-circuit wind tunnel. Commercial ANSYS Fluent program was used for numerical simulations. The k- $\epsilon$  realizable turbulence model, often applied for this type of tasks, was used in the calculations. As a result, distributions of the velocity amplification coefficient were obtained in the area under consideration, as well as images that present the averaged airflow direction. On basis thereof, potential zones where contamination accumulation may occur were determined.

The impact that introduction of a hypothetical high-rise building into the area would exert on wind conditions in its vicinity was also tested. High-rise buildings tend to intensify airflow in their immediate vicinity. Thus, they can improve ventilation conditions of nearby streets. However, in this particular case, the research prompted the conclusion that the proposed building causes turbulence and increased velocity gradients in the majority of elevation planes. On the other hand, in the ground-level zone, the building blocks rather than intensifies the airflow.

Keywords: smog; air pollution; aerodynamic; wind tunnel

### INTRODUCTION

In the context of city shaping, one of the important issues refers to the possibility of natural ventilation by means of ventilation corridors and by design of housing estates in such a way as to ensure that areas are ventilated by airflow. Unfortunately, the construction of ventilation corridors is subject to the pressure of financial capital. Therefore, housing estates are usually designed so as to maximize the use of the area available for development. The problem of smog and

the accumulation of pollution arises in densely built-up city downtowns, districts adjacent to them, as well as in towns that adjoin cities. Currently, more and more frequent measures are being introduced in Poland in order to reduce the scale of air pollution, especially in large urban agglomerations.

The topic has also become a point to be considered by scientists. Monika Fronczak of the Cracow University of Technology (M. Fronczak 2018) has presented

an extensive list of urban solutions. The analysis of the tools for city technological development proved technology to be an indicator of the city quality (C.E. Borrego *et al.* 2006). Jan Kiciński of the Institute of Fluid-Flow Machinery, the Polish Academy of Sciences, has developed 4 stages of implementing modern technologies in the municipal-housing development sector with which to reduce the emission of pollutants (J. Kiciński 2018). A comprehensive study on health consequences is presented books and articles (H. Mazurek and A. Badyda, 2018), (J. Schwartz, F. Laden and A. Zanobetti, 2002), (P. Dąbrowiecki *et al.*, 2021)]. Professor Andrzej Flaga of the Cracow University of Technology, together with his team, is working on an experimental city ventilating method with the use of ventilation towers and chimneys (F. Łukasz *et al.*, 2019). Moreover, futuristic visions may be found which, at present, are unlikely in realistic terms. These assume the use of pollutant-absorbing plants to cover entire facades of buildings (M. Khaled and K. Dewidar 2010). The location of a tall building has also been shown to affect the dispersion of pollutants in its vicinity (E. Aristodemou *et al.* 2020).

Air pollution is a complex issue. It depends on many factors, such as the source and geographic location. A less frequently considered but equally important feature consists in the aerodynamic factor, which may affect the concentration of pollutants depending on the shape of the building development.

Smog currently poses a large threat and is difficult to remove. The situation seems to be getting worse by the year. In order to tackle this problem, it is necessary to coordinate action in several fields simultaneously (E. Stanaszek-Tomal 2021). It is not enough to simply ventilate the city. Likewise, it is impossible to have most of the old-type heating burners replaced in single-family housing within a few years. Nor can the society (often poor (A. Michalak 2020)) be controlled on the use of ecological heating sources only. It is necessary to educate the society, introduce appropriate provisions of law that will hinder bad practices and facilitate good ones.

Architecture may provide great help in this aspect, because ultimately most of the pro-ecological activities are related to this discipline. It is also worth mentioning that architecture may be used as a huge propaganda tool already in the process of creating the design. Visualizations used by architects can reach the society easily, as recipients prefer information presented in visual form. The implemented project, in turn, provides the final evidence of the seriousness of the problem and serves as proof of the legitimacy of the actions taken. If buildings are shaped with ecology in mind, education of the society will progress much faster.

Unfortunately, the phenomenon of air pollution in cities has not been thoroughly investigated. In Poland, large gaps in the location of measuring stations may be observed, which results in large information gaps. There are about 260 stations (P. Kleczkowski 2019), only 8 of which are placed in the city of Warsaw: 4 of them are automatic, 3 automatic-manual and 1 is manual only (Generalna Inspekcja Ochrony Środowiska, no date). Pollution measurements give an opportunity to examine the degree of pollution, but only so at the measurement station itself. Such stations, however, are installed near the ground floor. Both, the composition and intensity of air pollutants changes with height and vicinity of the test site. The result will, thus, be different at the height of the 10th floor, at the level of the ground floor, and different, still, in the buildings dispersed in suburban areas. The air condition is influenced by many factors, including the type and severity of aerodynamic phenomena. For a more accurate prediction of air pollution, it is necessary to study aerodynamic phenomena in the context of building developments. It is also indispensable to measure such phenomena with the use of a more densely located grid of measuring stations located at different heights. This implies the need to create a pollution map in 4D. The map would be developed over time (T. Villa *et al.* 2016), and would account for variables such as, for example, aerodynamic phenomena depending on the wind direction. It is impossible to create such a map solely on the basis of stationary pollution measurement stations, even if the quantity of such stations increased.

Drones are devices that can be used to measure pollution (S. Szymocha and J. Osuchowski 2019), (O., no date), (S. Duangsuwan and P. Jamjareekulgarn 2020), (T. Landolsi *et al.*, 2019). Such measurements are already taken with the use of small and light aircraft (C.E. Corrigan *et al.* 2008). Components such as smog sensors, chemical and radiological sensors can be attached to such a device. With the use of drones, the level of dust and gases can be monitored, weather data can be collected or high-voltage electricity lines may be diagnosed (S. Szymocha and J. Osuchowski 2019).

In the context of the issues raised in the present paper regarding the deposition of pollutants in the city area, it seems important to identify potential air stagnation zones that favor the accumulation of dust and gases.

Following the above premises, the authors examined an exemplary area of urban building development. The building is located in the center of Warsaw and is intersected with one of the city's busiest communication routes. The research was aimed at determining the potential zones of pollution accumulation in the

dense building development of the city (marked with a red circle in Figure 1). The selection of such zones seems advisable, because in the least ventilated places it would be possible to take most accurate measurements under real conditions.

Moreover, it was intended at investigating the impact of introducing a high-rise building (196 m in height, highlighted in blue on the map below) on the ventilation conditions located in its vicinity (T. Stathopoulos 2009), (T. Stathopoulos 2011), (Q. Xia *et al.* 2013). A high-rise building tends to intensify the airflow. It can, therefore, improve the ventilation conditions in its immediate vicinity. However, in the winds of higher velocities it can be a source of discomfort to pedestrians.

## 2. MATERIALS AND METHODS

### 2.1. Urban-planning analysis

The surroundings of the studied area are not fully developed under Miejscowy Plan Zagospodarowania Przestrzennego (MPZP). The only valid MPZP Plan No. XCIV / 2749/2010 of November 9, 2010 (Rada Miasta Stołecznego Warszawy, 2010), concerns the immediate surroundings of the Palace of Culture and Science. The Plan allows for the construction of buildings within the range of 24-26m in height, with the possibility of designing a high-rise building development part within the range of 233-245m. The immediate surroundings of the Złota 44 building, around which the present research is centered, is not covered by the Local Development Plan (MPZP). Changes to this space are difficult to predict, as building permits may currently be issued on the basis of the Decyzja o warunkach zabudowy [Decision on Development Conditions], the content of which depends on the civil servants who issue the document. For the purposes of the present publication, it can be assumed that the area will not undergo significant changes over the next 5-10 years.

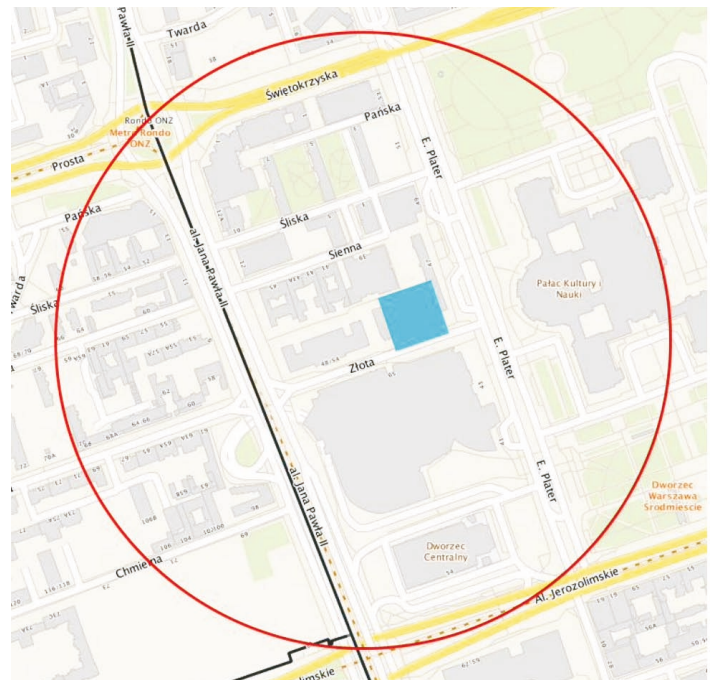
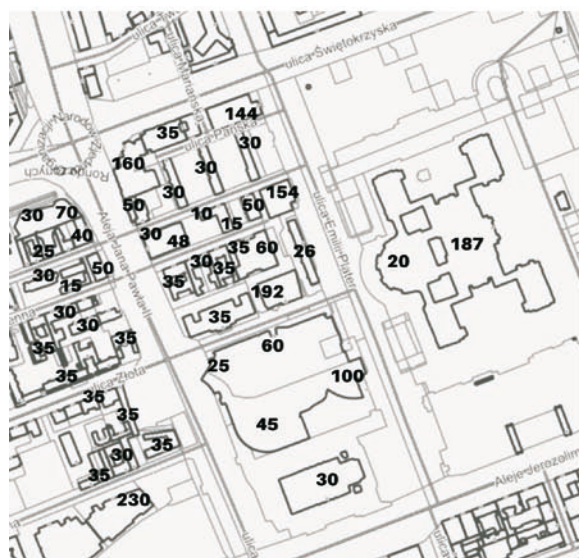


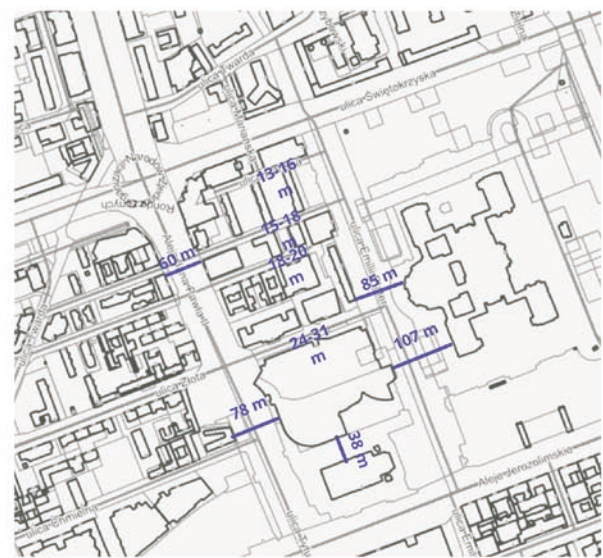
**Fig. 1.** Study area including the proposed building - the radius of the circle equals 300m (author's own study)

The area under study covers about 43 ha. It is intersected by a grid of streets oriented south-west-north-east (Aleje Jeruzolimskie, Złota Street, Sienna Street, Śliska Street, Pańska Street, Świętokrzyska Street) and north-west-south-east (Aleja Jana Pawła II, Emilii Plater Street). The present research analyzes were confined to the street quarter marked by the following streets: Emilii Plater, Aleje Jeruzolimskie, Aleje Jana Pawła II and Świętokrzyska. Architectural forms that occur in this area vary (Fig.1). These include densely developed tenement houses, high-rise buildings and more extensive volumes, such as the Złote Tarasy Shopping Center (ZT) and the Palace of Culture and Science. The heights of buildings and the widths of individual street canyons are shown in Fig. 2. Due



**a**

**Fig. 2.** Analysis of the height of buildings (a) and the width of street canyons (b) in the studied area (author's own materials)



**b**

to the lack of access to accurate data on buildings, they were determined by means of comparison to the heights reached by the authors during an on-site visit and by analyzing 3D models in Google Earth. Accuracy of up to 5m was assumed. The widths were measured on the City of Warsaw website, with the use of an interactive map featuring the ability to measure distances. The results were confirmed during an on-site visit.

## 2.2. Geometry of the tested layout

In Fig. 3, the actual set of models tested experimentally together with the high-rise building marked with the letter X in the illustration is presented. The mock-up for the research was made in the 1: 700 scale.

The next illustration (Fig. 4) shows the full set of models subjected to numerical analysis. This analysis was aimed at examining the influence of the high-rise building, marked with the letter X in Figure 3, on the wind conditions in its immediate vicinity. Compared to the model tested in the wind tunnel, two main differences occur in this case. Some of the obstacles, distant from the building important from the perspective of the present paper, or located on its leeward side for the studied wind directions, were excluded from the analysis. These buildings are marked in gray in Fig. 3. The second difference concerned the simplification of the group of buildings, marked with a blue rectangle in Figure 3, to four cuboids, while maintaining the height of the buildings and the spacing (understood as streets) between them.

According to the authors, the simplifications had little impact on the results obtained in the vicinity of

building X and significantly shortened the computation time.

### *Description of the research methods applied*

Research on airflows around building, which are commonly used and described in the literature (B. Blocken, T. Stathopoulos and J.P.A.J. van Beeck 2016), may be divided into experimental ones (conducted in a wind tunnel) and numerical ones. The most reliable results are obtained by combining both types of research. The results of experimental research offer a chance for a general identification of phenomena, enable researchers to specify problem areas and constitute the basis for determining the parameters entered into computer programs.

The experimental research was conducted in a through wind tunnel whose cross-section equaled 1m. by 1m., with a closed measuring space of the same dimensions. The wind structure at ground-level was created by modeling the velocity profile and turbulence intensity distribution according to PN-EN 1991-1-4: 2008 (N.E. En and P. Normy 2008) and the procedure described in (M. Jedrzejewski, M. Pocwierz and K. Zielonko-Jung 2017) the velocity profile was obtained from the formula:

$$\frac{V}{V_{10}} = \left(\frac{z}{10}\right)^{0,24} \quad [1]$$

where:  $V_{10}$  – wind velocity at a height of 10 m. above the ground (m/s),  $z$  – height above ground level in m.

Such a velocity profile corresponds to the characteristics of dense building development located in

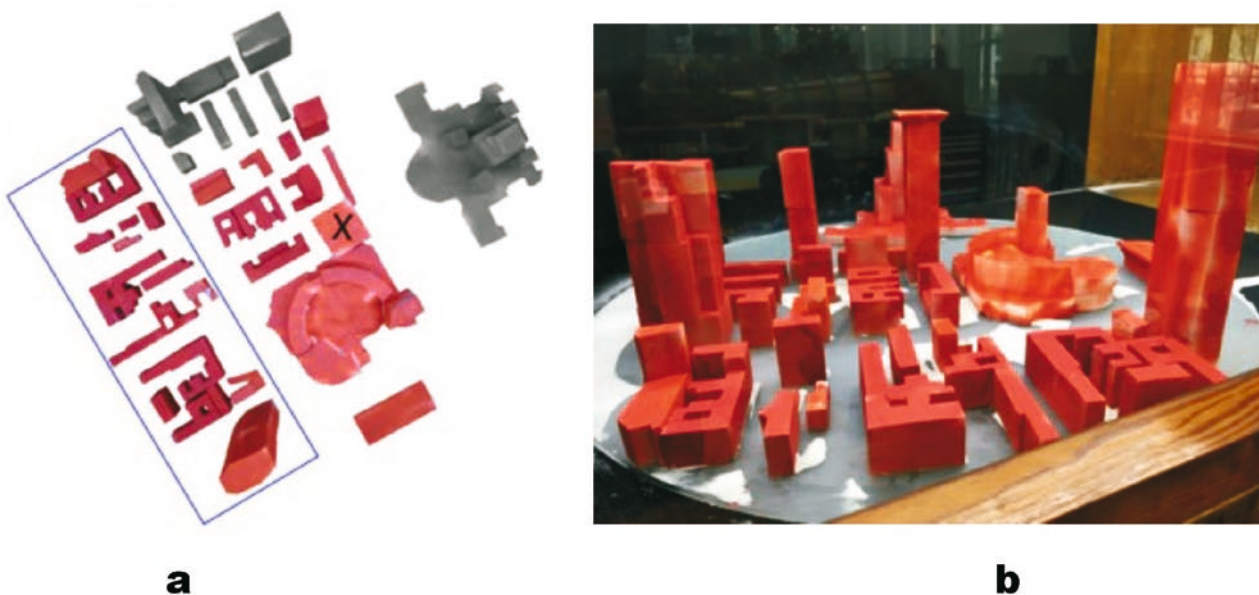


**Fig. 3.** Model for experimental tests - high-rise building marked with the letter X (a) and a photo of the model used for experimental tests (b); source: by the authors.

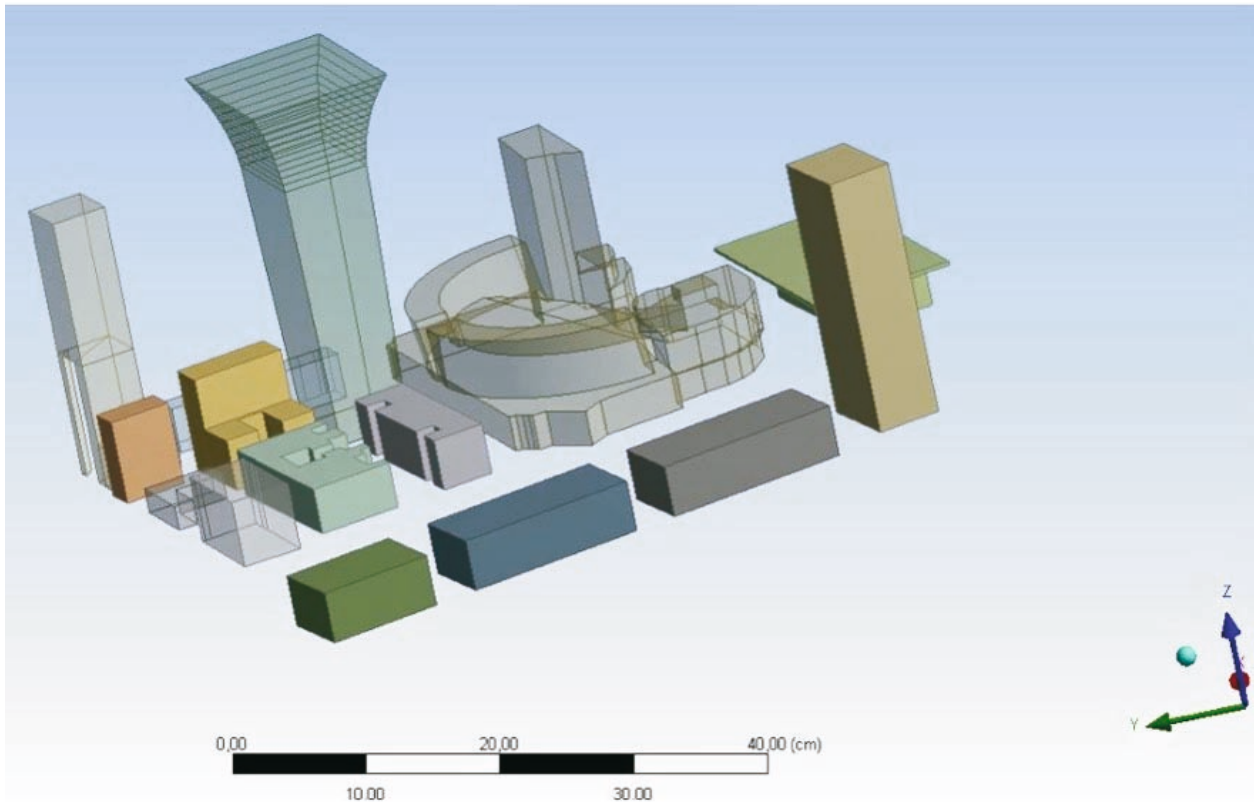


**Fig. 4.** The full set of models subjected to numerical analysis in the 1: 700 scale; source: by the authors

large cities. The intensity of turbulence was calculated on the basis of the formula -  $lv(z) = 1/\ln(z/z_0)$  (assuming a unit value for  $z_0$ ).

In order to model the ground layer, elements to disturb the airflow and roughness elements in the form of spiers and blocks were installed in the tunnel. These objects were placed at the base of the tunnel in front of the study area with model building developments. The results of average velocity profile measurements and intensity of turbulence at the altitude of up to 100 m. were quite consistent with the desired characteristics.






For the research conducted for the purposes of the present work, the Reynolds number was approximately  $3 \cdot 10^5$ . In actual flow, the number value is higher by several orders. In tunnel research, it is very difficult to obtain the actual Reynolds number. However, for sharp-edged objects, the airflow undergoes high turbulence, detachments and vortices occur. Therefore, airflow is relatively insensitive to the Reynolds number (P. Irwin, D. Scott, R. Denoon 2013). Airflow distortion and the resulting changes in pressure distribution can be treated as negligible for Reynolds numbers higher than  $10^5$  (D. Duthinh and E. Simiu 2011). Methods for ground-level modeling similar to the ones used

in the quoted studies have described in (B. Blocken, T. Stathopoulos and J.P.A.J. van Beeck 2016), (K. Gumowski *et al.* 2015), (J. Sanz-Rodrigo, J.P.A.J. van-Beeck, G. Dezsö-Weidinger 2007), (S. Reiter 2010) and elsewhere.

Two methods were used in tunnel studies, that is oil visualization and sand erosion method (B. Blocken, T. Stathopoulos and J.P.A.J. van Beeck 2016). Both methods are of qualitative nature. Their purpose is to arrive at a good understanding of airflow phenomena that occur in a given area and to form some intuitive assumptions concerning acceleration or deceleration of airflow for given data on building layouts, rather than to obtain accurate quantitative data.

A mixture of oil and titanium white is used for oil visualization. The mixture is applied onto a plate made of black glass to which models of buildings are attached. During the tunnel experiment, oil is blown off areas of high airflow velocity and accumulates in areas where airflow is much less intense. The procedure results in an image showing the averaged direction of airflow, while the layouts of the oil streaks show the turbulence pattern in the flow. During the experiment, photos are taken (around 60-70 photos taken approximately

**Table 1.** List of symbols used in the study, together with their interpretation

Designation on the oil visualization map	Name of form	Description of flow structure
	Stagnation zone	Stagnant zone. Places where air moves very slowly are often found in confined spaces between buildings or in the footprint behind large buildings
	Direction of flow	Velocity vector of moving air
	Air reflected from the building on the windward side	Some of the air encountering the bouncing obstacle descends toward the ground and then changes its direction to the opposite of the incoming stream. This creates a horseshoe vortex
	Contractual limit of reflected air	Places where reflected air meets incoming flows. This is a conventional boundary because it is often not clearly visible and its location can only be estimated
	Whirl	Indicates a recirculation zone. Whirls often form on the leeward side of the building.

Source: prepared by the authors

every 10 seconds). The analysis of photo sequences prompts the understanding the phenomena that occur in airflow and interpretation thereof.

The Table 1 above presents a list of symbols used in the description of visualization tests, together with their interpretation.

The second experimental method used in the described research was sand erosion method, presented in detail in (B. Blocken and J. Carmeliet 2004), (S. Reiter 2010). It uses sand with a standardized diameter and a very low humidity coefficient. The saltation test consists of two stages. Firstly, the reference velocity is determined at which the layer of applied sand is almost completely blown off the plate. Velocity is measured with a Prandtl tube in an undisturbed area, at some distance from the ground. The second stage consists in the actual measurement. In this case, building models are placed on a roughened slab, whereas sand is evenly applied to the empty areas between the buildings. The test is performed in a tunnel where the velocity is gradually increased by  $\Delta v$  to reach successive values. After each change of velocity, it is neces-

sary to wait a while for the airflow to stabilize and for the sand to cease erosion, and then photos of the test area can be taken.

The photos for the following velocities are processed and superimposed over one another. As a result, a color map of the airflow velocity amplification coefficient -  $\alpha$  is obtained. To determine the value of the coefficient, both reference velocity and the one that is set at the test moment must be known.

For the tested building layout, the following amplification factors  $\alpha$  were obtained, which were assigned to separate colors (Fig. 5).

Knowing the undisturbed airflow velocity from a given direction (e.g., from meteorological measurements), it is possible to estimate the values of velocity at each point of the test area based on of the map obtained from sand erosion study. If velocity at a given height in the undisturbed area is  $v$ , then the velocity at a specific point in the area at that height may be obtained from the formula:  $w = \alpha \cdot v$ . As it can be seen, for the obtained amplification coefficients, airflow velocity in the areas marked in red reaches values above



**Fig. 5.** Legend that explains the color scheme depending on the amplification coefficient, by the authors

5 m/s at the wind velocity value slightly above 3 m/s. These places are well ventilated and retain low level of susceptibility to the accumulation of contamination. Moreover, the opposite effect of building development on wind conditions may be observed - places where the obtained amplification coefficient reaches values of less than 1 are areas of a reduced airflow velocity. Zones where the air slows down significantly (marked in navy blue and black) present potential stagnation zones where pollutants are likely to accumulate due to obstructed ventilation.

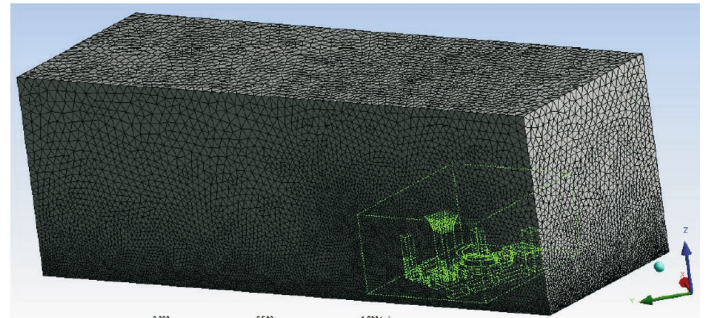
The ANSYS Fluent software was used for numerical simulations of the flow in the presented built-up area. First, the geometry and computational grid were created, in accordance with the recommendations contained in source literature (M. Jedrzejewski, M. Pocwierz and K. Zielonko-Jung 2017), (S. Reiter 2008), (S. Reiter 2010), (B. Blocken *et al.*, 2011), (J. Franke *et al.* 2007), (Y. Tominaga *et al.* 2008).

Figure 6 presents an example of a computational domain with a grid. The domain cross-section reflects the cross-section dimensions of the wind tunnel in which the material model was tested. The length of the computational area equaled 3 m.

The grid consisted of 8 million tetrahedral elements. These were highly densified in vicinity of the building models and near the ground surface, whereas they gradually thinned out in each direction. The volume ratio of adjacent elements was reduced to 1.05.

In order to compare the obtained results, calculations were also conducted for a more densified computational mesh that consisted of 14 million elements. No significant differences in the obtained results were noted.

The RANS model was used for the simulations in Fluent, in accordance with guidelines contained in the article (B. Blocken, T. Stathopoulos and J.P.A. J. van Beeck 2016). The *pressure-based solver* type was chosen, owing to the fact that air is considered incompressible at low flow velocities (and it is with such velocities that air moves in the ground zone). The *SIMPLE* algorithm was applied, based on the *segregated* method. To discretize the equations of momentum, kinetic energy and turbulence energy dissipation, first-



**Fig. 6.** An example of a computation grid in a selected calculation domain with the layout geometry placed inside of it; by the authors

order equations were used for the first several tens of iterations, and later the *second order upwind* was applied. This technique is widely used and described in source literature (J. Franke *et al.* 2007). Its aim is to minimize the time required in order to perform calculations, while maintaining the precision thereof. The *k- $\epsilon$  realizable* model of turbulence was adopted, which was selected based on source literature (Blocken, Stathopoulos and van Beeck 2016), (K. Gumowski *et al.*, 2015). Moreover, in order to calculate airflow parameters in vicinity of obstacles, it was decided to use *Standard Wall Function*. This option does not require a particularly dense computational grid in the immediate vicinity of buildings, which offers a chance for optimization in terms of the computing power used. The velocity profile was implemented into the program using a function written in C language.

### 3. RESULTS

Both tunnel research and numerical simulations were conducted for two wind directions - west and south-west winds. (Fig. 7) The selection of directions was made based on the analysis of the wind rose for Warsaw (International Renewable Energy Agency, no date) and the average distribution of airflow velocity for Warsaw at a height of 10 m. The analysis shows that winds from the above-mentioned directions dominate in area under consideration.

**Table 2.** Table of wind directions and velocity in Warsaw

Wind velocity, m/s	Wind direction							
	N	NE	E	SE	S	SW	W	NW
Average velocity	4,0	3,7	4,0	3,4	2,8	3,4	4,6	4,4
max velocity	15	13	13	13	13	15	20	20

Source: International Renewable Energy Agency, no date)

Additionally, oil visualizations and sand erosion methods were applied to research the east, north and north-west directions.

The above table (Tab. 2) presents average and maximum wind velocity for the city of Warsaw, estimated on the basis of frequency and probability distribution for wind velocity at a height of 10 m. for the Okęcie area.

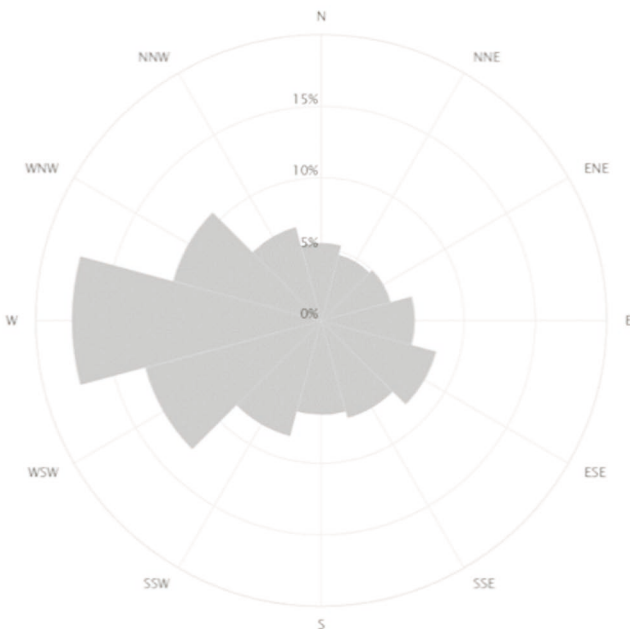


**Fig. 7.** Wind rose for Warsaw and the surrounding area; source: International Renewable Energy Agency, no date)

The values of average airflow velocity for the west and south-west wind directions were converted to the pedestrian level values and equal 3.02 m/s and 2.24 m/s, respectively.

*The analysis of air flow in a built-up area for the west direction*

Experimental and numerical studies for the west wind direction were conducted for two configurations of the area under consideration. The first configuration has no buildings, whereas for the second one, a high-rise building is introduced (marked with X in the pre-

sented figures). Its parameters are discussed in chapter two.

The results obtained during the sand erosion study for the west direction for both building configurations are presented in Fig. 8a (the building is not presented) and Fig. 9a (the building is presented). The results obtained in the oil visualizations in Figs. 8b and 9b, respectively. Based on the analysis thereof, it can be concluded that both in the area under consideration without the X building and with the X building, the zones where reduced wind velocities occur are located between the buildings 20 and 19 (when viewed from above), on the leeward side of the buildings 18 and 17, and inside the courtyard and behind the building 16. They can also be observed between the buildings 11 and 10 and 8 and 7, in the quarter formed by buildings marked with numbers 1, 4 and 3, as well as on the leeward side of the building development line marked by the buildings 13, 5, 2, ZT (Złote Tarasy) and PKP (Polskie Koleje Państwowe). As mentioned above, the amplification coefficient for these zones amounts to less than or equal to 0.64. Therefore, the actual average airflow velocity in the area in question is unlikely to exceed 2m/s. Undoubtedly, zones of reduced velocity value, but not in direct vicinity of the leeward wall of buildings or building corners, namely where vortices and turbulence occur, may be seen as places where unmanned aerial vehicles can be used for air pollution measurements.

Considering the presence and influence of the high-rise building marked with the letter X in the figures, it can be noticed that for the west direction, the X building hinders the airflow between buildings ZT and 1, which exerts a key impact on the emergence of stagnation zones. The presence of the X building has a positive effect on the ventilation of the stagnation area behind the ZT and PKP facilities. At the same time, however, it building hinders the airflow in the vicinity of the Palace of Culture and Science, and around the buildings 2 and 5. Ventilation of the space between the buildings 1 and 4 is also worse when the X building is present.



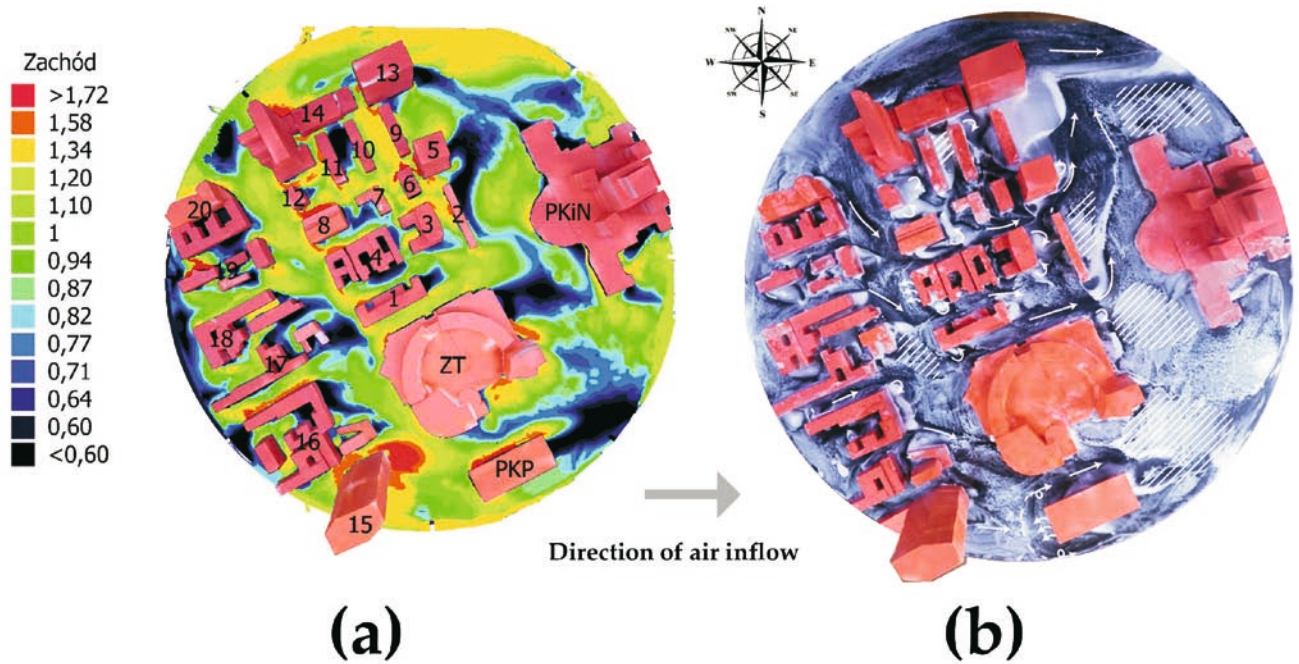


Fig. 8. Sand erosion study map (a) and oil visualization (b) for the west direction without a building; prepared by the authors

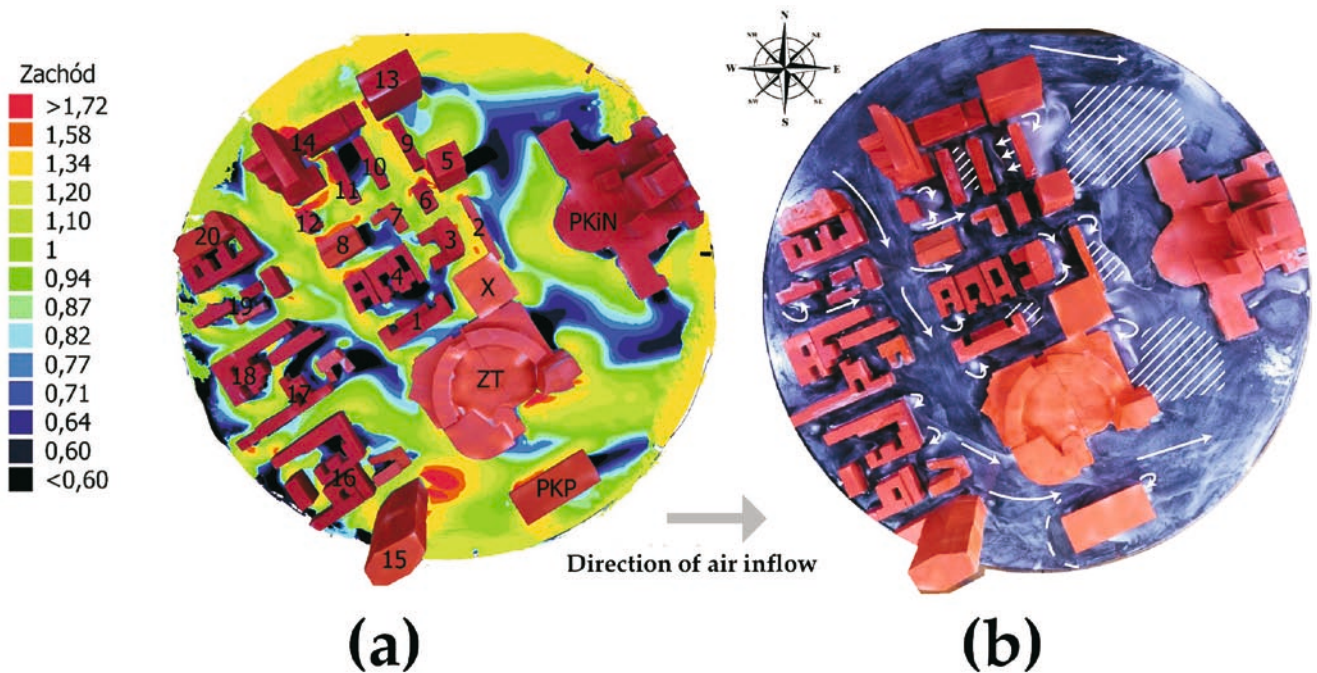


Fig. 9. Sand erosion study map (a) and oil visualization (b) for the west direction with a building; prepared by the authors

Due to the simplification of the geometry in the area under consideration, the results obtained from numerical simulations (Fig.10) differ from the results of experimental studies, although similarity in the general nature of the flow is retained. A significant difference is observed on the leeward side of the buildings designated by buildings number 2, 5 and ZT. This results

from the fact that the existence of the Palace of Culture and Science was not taken into account in the calculations. This is a building of significant height, thus the airflow in its vicinity is intensified. This fact can be easily observed by comparing the amplification coefficient maps obtained from experimental tests (Fig. 8,9) and numerical tests (Fig. 10).

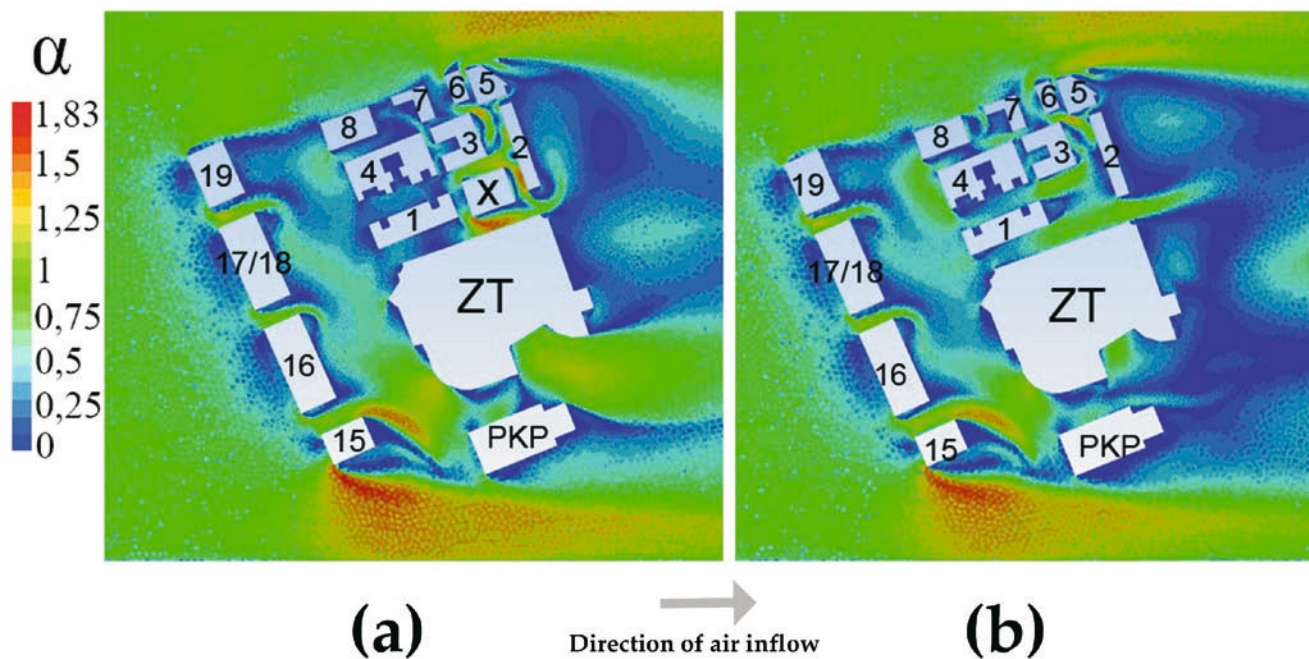


Fig. 10. Numerical result - comparison of air velocity at the level of 2.5 mm with (a) and without the building (b); prepared by the authors

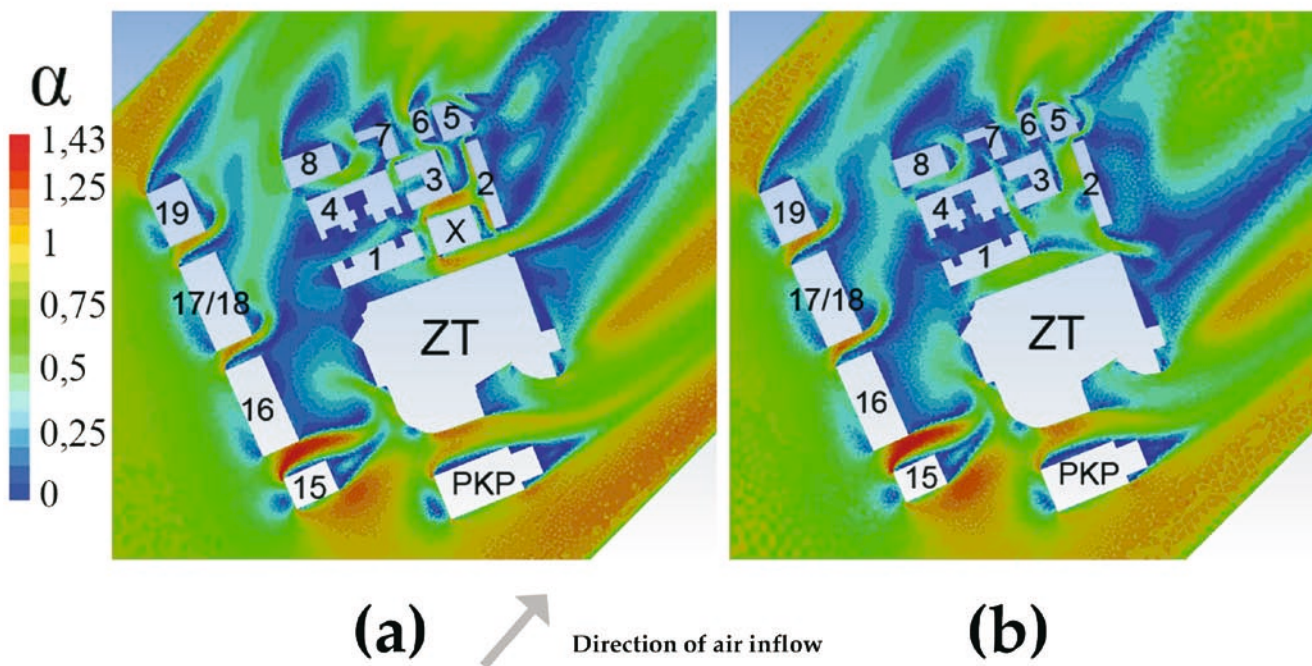
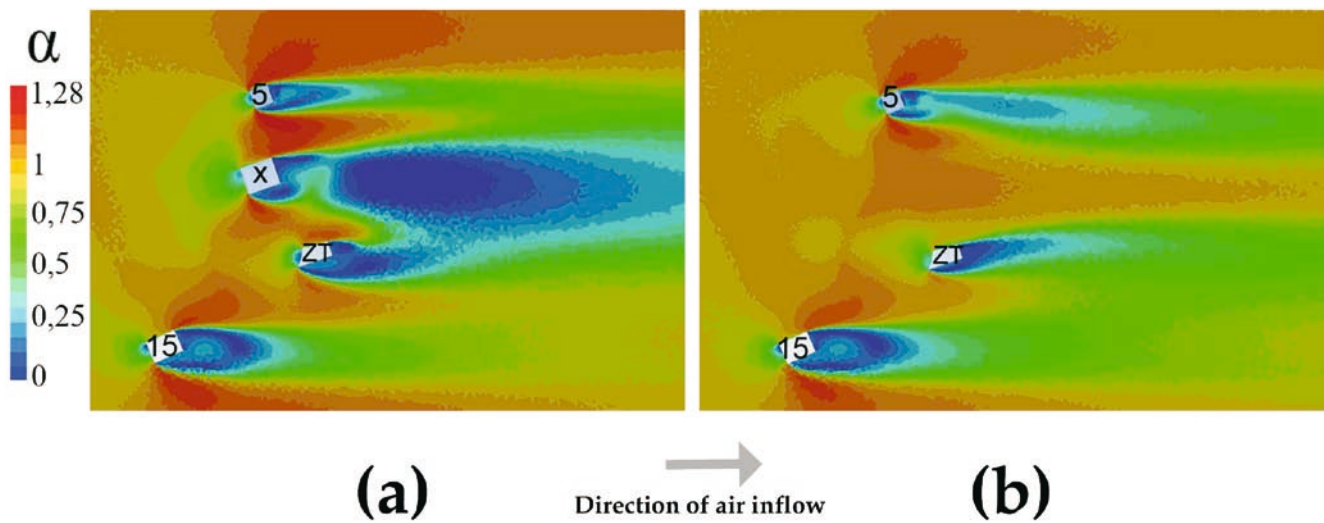


Fig. 11. Numerical result - comparison of air velocity at the level of 10 mm with (a) and without the building (b); prepared by the authors

However, when analyzing the situation, especially in the rectangle located in the center of the area, on the leeward side of the building development line defined by the buildings 15-19, many similarities can be noticed. Moreover, the values of the amplification coefficient do not differ significantly from the values obtained in experimental research. Numerical research provide insight also into the zone between the X build-

ings and ZT at lower heights. Owing to the shape of the X building, this area is completely covered in the photos taken during sand erosion study and oil visualization.

Fig. 10 illustrates the velocity values at specific spots between buildings at a height corresponding to the pedestrian level (2.5 m in high in the domain in question, which matches 1.75 m in the actual area).



**Fig. 12.** Numerical result - comparison of air velocity at the level of 100 mm with (a) and without the building (b); prepared by the authors

Furthermore, numerical studies make it possible to observe airflow in the area under consideration at altitudes above the pedestrian level. Exemplary maps of the amplification coefficient distribution are presented in Figures 11 and 12. Respectively, the maps are made at a height of 10 mm. in the model scale, which corresponds to 7 m. in an actual scale and at a height of 100 mm., with matches 70 m. in actual conditions.

In principle, no alteration to airflow was observed at a height corresponding to 7m., as compared to the pedestrian level (1.75m).

On both levels (namely 1.75 and 7 m.), the impact exerted by the introduction of the X obstacle into the building complex is clearly visible, which is reflected in the ventilation of the area to the south-east of the building marked as ZT. This phenomenon was also no-

ticed for the sand erosion and oil visualization studies. The X building obstructs the air flow between the ZT building and the buildings marked as 1, leading to the reduction in airflow velocity in this area. At the same time, between the X building and ZT building, the amplification coefficient increases.

At low heights (up to 10 m.), the wind conditions in vicinity of high-rise buildings, namely the building 15 and the X building (if introduced), tend to be the least favorable. Additionally, in the presence of X building, the space between the ZT and the PKP buildings may cause dangerous acceleration to airflow.

In Fig. 12 the map of the amplification coefficient is presented at a height of 100 mm. above the ground in the model scale, which corresponds to the height of 70 m. in the actual scale. At this height, only buildings

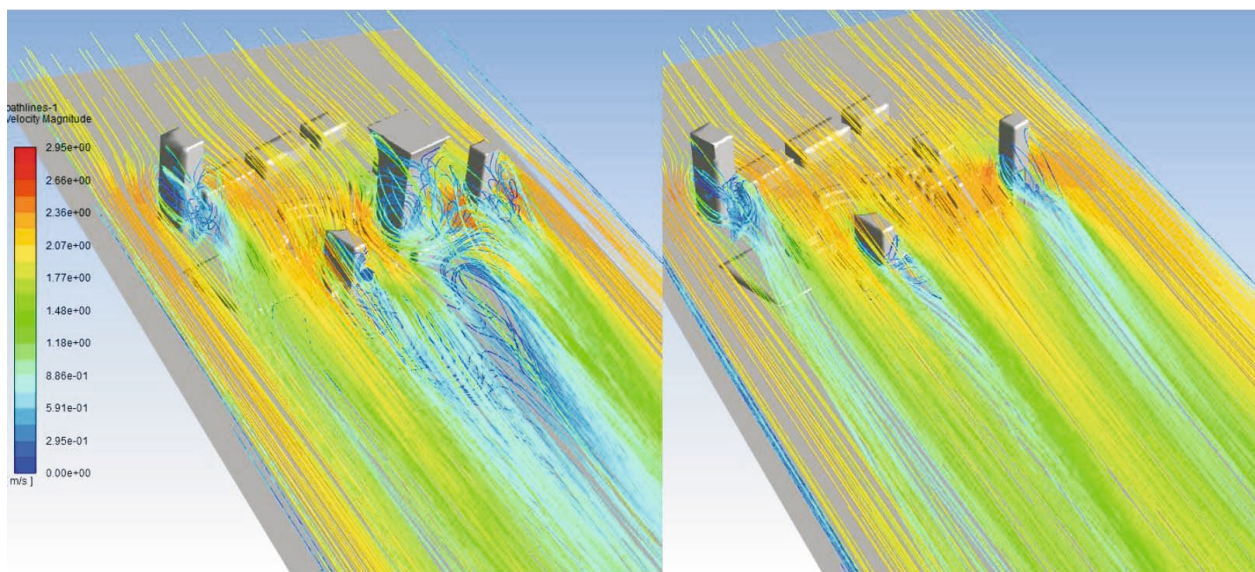


**Fig. 13.** Comparison of the streamline at a height of 100mm in the presence of building X (a) and its absence (b); prepared by the authors

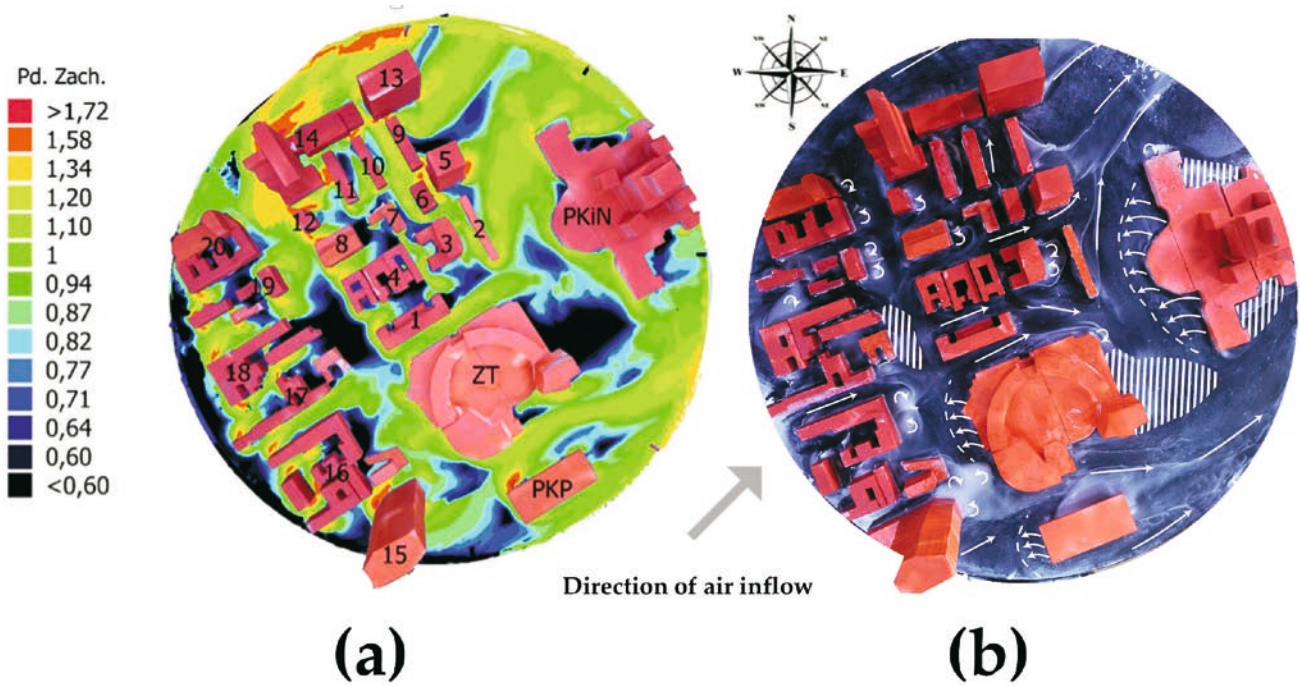


Fig. 14. Sand erosion study map (a) and oil visualization (b) for the southwestern direction without a building; prepared by the authors

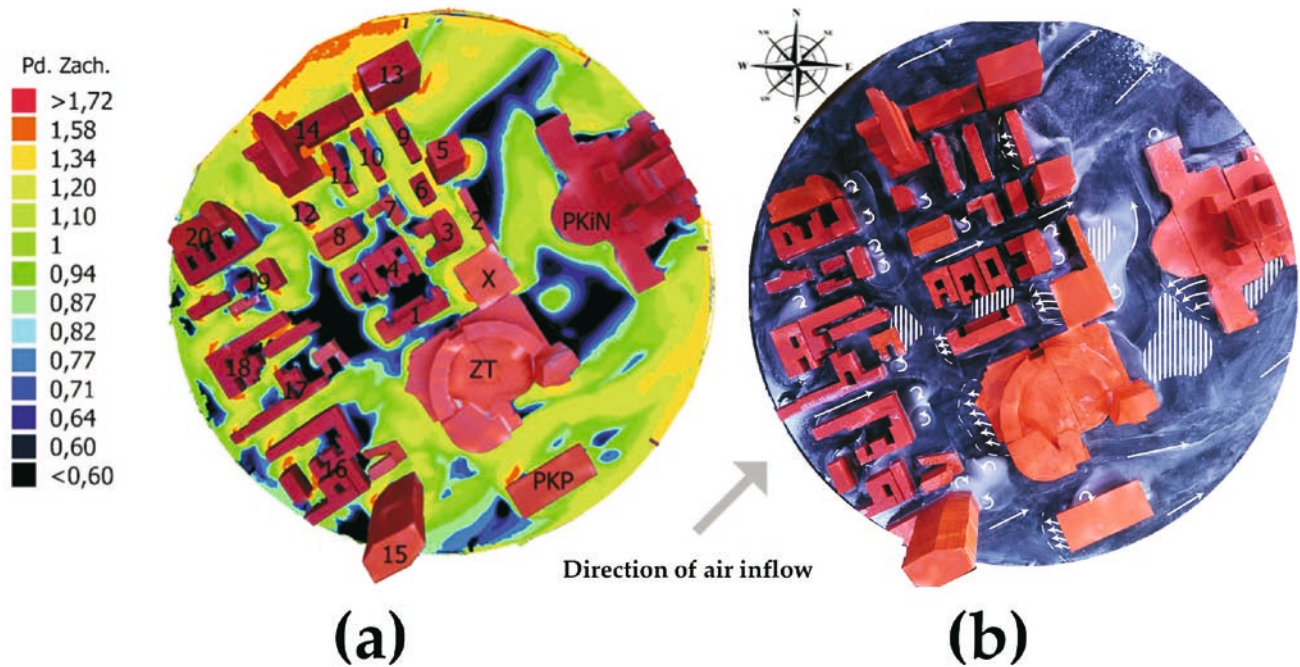


Fig. 15. Sand erosion study map (a) and oil visualization (b) for the southwestern direction with a building; prepared by the authors

marked as 15, ZT and 5, as well as the conceptual X building are visible. It can be seen that the airflow between the buildings accelerates, while behind the buildings zones of reduced velocity value are observed. In this case, the impact exerted by the introduction of X building is noticeable.

*Analysis of air flow in a built-up area for the south-west direction*

As in the case of the west wind direction, two configurations of building development were investigated – when the X building is absent and with its presence. The results of the sand erosion study are presented in Fig. 14 and 15, whereas the outcomes of the oil visualization are shown in Fig. 14 and 15.

For the south-west direction, for which average airflow velocity at the height of the passerby for undisturbed flow is estimated at 2.24 m/s, in the zones marked in navy blue the velocity decreases to a value equal to or lower than 1.34 m/s

The largest zones of reduced velocity, both for the variant with the X building and without it, were observed behind the 18 and 17 building complexes, as well as behind the building marked as ZT.

However, relatively few zones where the velocity is significantly increased were noted. Such zones appear mainly at the building corners, whereas the velocity amplification barely exceeded the value of 1.58. It is, thus, estimated that for south-west winds, the average velocity at pedestrian level should not exceed 3.5 m/s.

The introduction of the X building resulted in a partial blockage of the aerial corridor between the ZT and the building 1, as well as it led to stagnation towards the east of the building 2.

Moreover, when the X building is present, the air accelerates at its base, especially from the windward side, where a zone reflected air in the shape of horse-shoe vortex is created.

To summarize in brief, for the south-west direction, the X building again led to hindering the air flow between the ZT and the building 1. This had an impact on the emergence of stagnation zones on the windward side of the Palace of Culture and Science. It is difficult to associate the presence of the X building with any positive phenomena that would occur in the airflow between the studied buildings, as compared to the situation when this building is absent. The flow intensification took place only in the close vicinity of the windward side of the building, it failed to contribute to better ventilation of the streets in the vicinity of the building.

The results of numerical calculations for the incoming air from the south-west direction are presented in Fig. 16, 17, Fig. 18. In this case, a slowdown can be observed within the aerial corridor delineated by buildings ZT and 1 in the case of introduction of the X build-

ing. With reference to the leeward side of the building 2, it can be noticed that negative impact in the form of a stagnation zone that forms in this area is exerted by the presence of the X building. This situation is also very well visible in the results obtained from experimental studies, that is sand erosion and oil visualization. As with a west wind direction, the visualization of the airflow at 10 m. (equivalent to 7 meters in actual conditions) is similar to the flow at pedestrian level.

Fig. 18 shows the distribution of the flow velocity amplification at height of 100 mm. (equivalent to 70 meters in actual conditions) around building models with and without the conceptual X building. Again, the introduction of the X building is strictly related to the emergence of a zone with increased turbulence. Moreover, the air bounced off the X building is partially directed to the right when viewed from the windward side and leads to the reduction in the effect of the higher part of ZT on increasing the velocity gradient in its wake.

*Analysis of the influence of the X building on the air flow in the built-up area for other selected wind directions*

This part of the chapter contains selected results of experimental studies for inflow directions that occur less frequently in actual conditions. The figures below show oil visualization maps for the air flowing in from the south (Fig. 19) and sand erosion for the north-west direction (Fig. 20).

In the case of a south wind (Fig. 19), a slight influence exerted by the X building on the flow can be observed. This situation results from the fact that for this direction airflow is in the wake of a large ZT object. Therefore, less air at high velocity reaches the building, while its trajectory could be influenced. Numerous similarities between the two maps have been observed, namely the main flow directions, stagnation zones and vortex zones are largely the same.

In the case of the north-west (Fig. 20) direction of the air inflow, it can be noticed that the X building is located in the zone where, in the absence of the X object, air stagnation occurs. Being a high-rise obstacle, the building results in bringing some of the airflow downwards from the upper layers. Therefore, the space in the immediate vicinity of buildings marked with numbers 2 and 3 is ventilated. Moreover, in the air corridor between the buildings 2, 5, 13 and the Palace of Culture and Science, the airflow tends to be slightly faster. This may be due to the introduction of the X obstacle, whereby the flow increases its velocity in unbuilt spaces. Moreover, it is worth noting the fact that when the X obstacle is removed, a stagnation zone forms instead. Contaminants that would otherwise be removed by wind may accumulate in the zone.

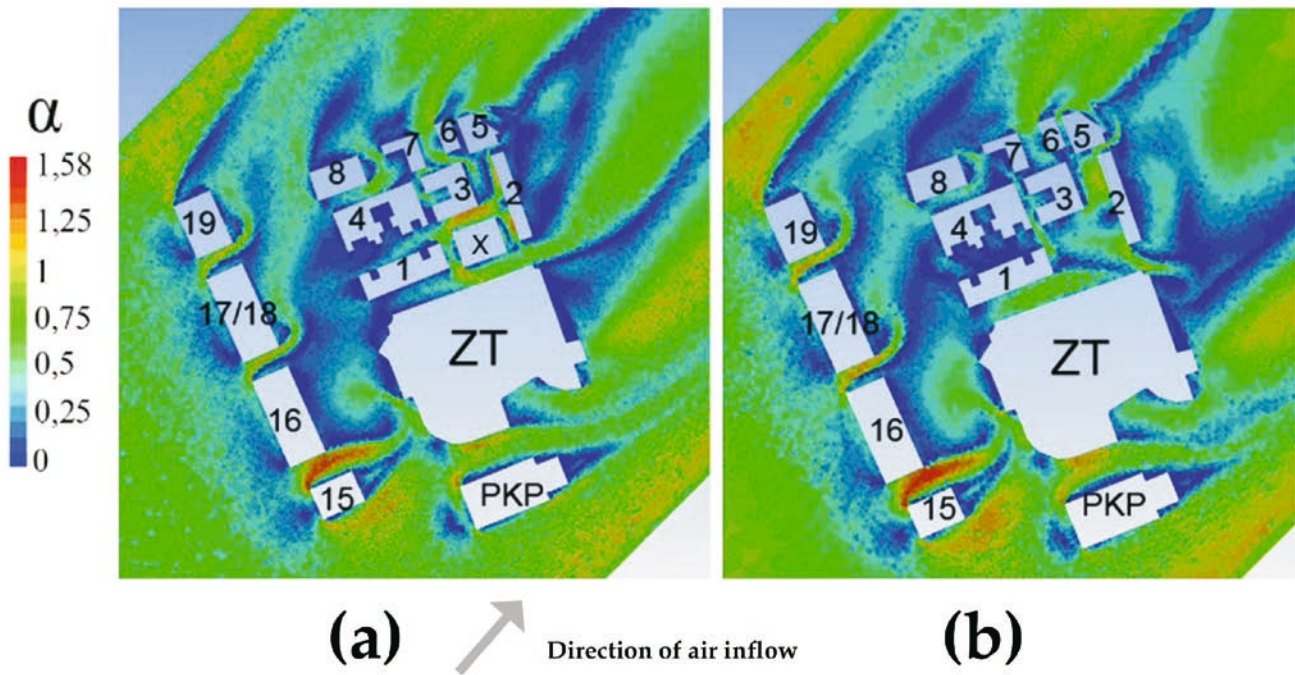


Fig. 16. Numerical result - comparison of air velocity at the level of 2,5 mm with (a) and without the building (b); prepared by the authors

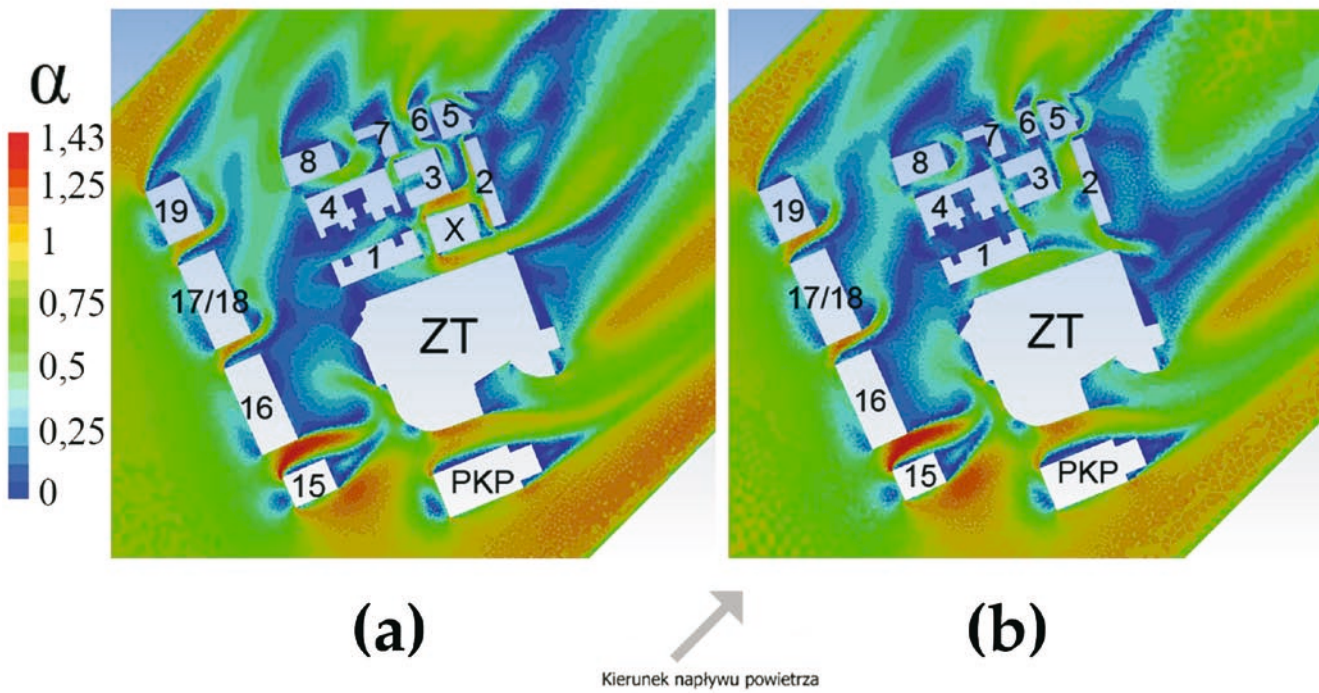
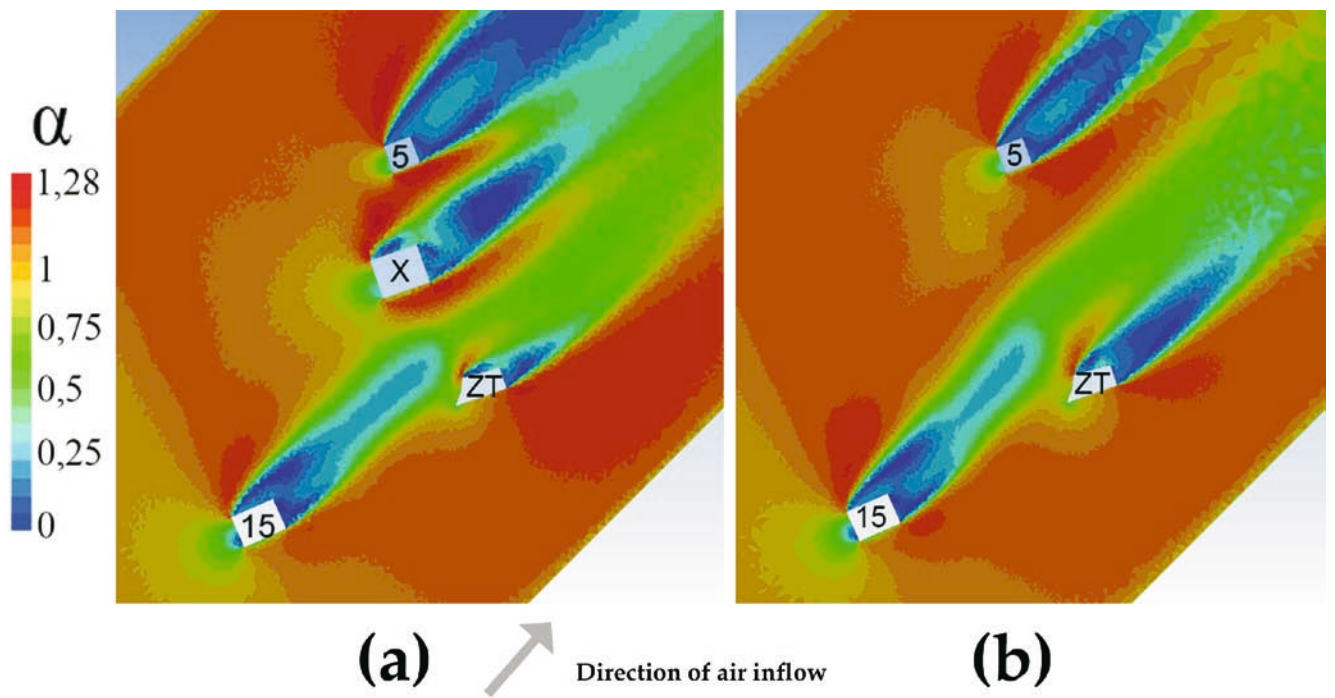
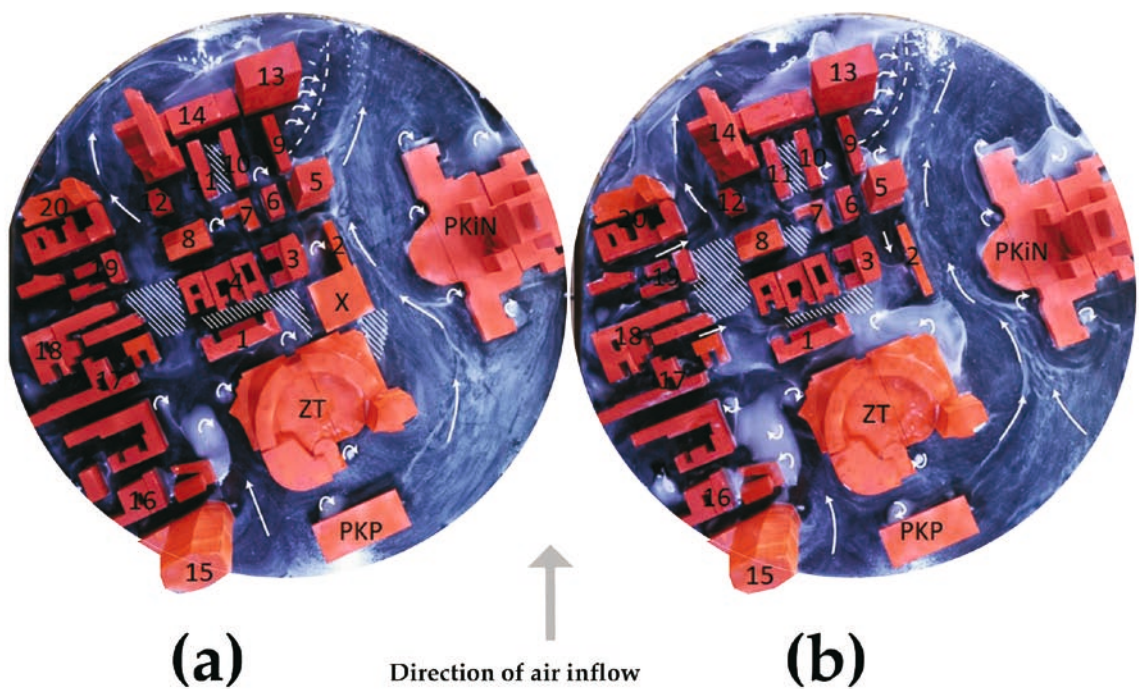


Fig. 17. Numerical result - comparison of air velocity at the level of 10 mm with (a) and without the building (b); prepared by the authors



**Fig. 18.** Numerical result - comparison of air velocity at the level of 100 mm with (a) and without the building (b); prepared by the authors



**Fig. 19.** Numerical result - comparison of air velocity at the level of 100 mm with (a) and without the building (b); prepared by the authors

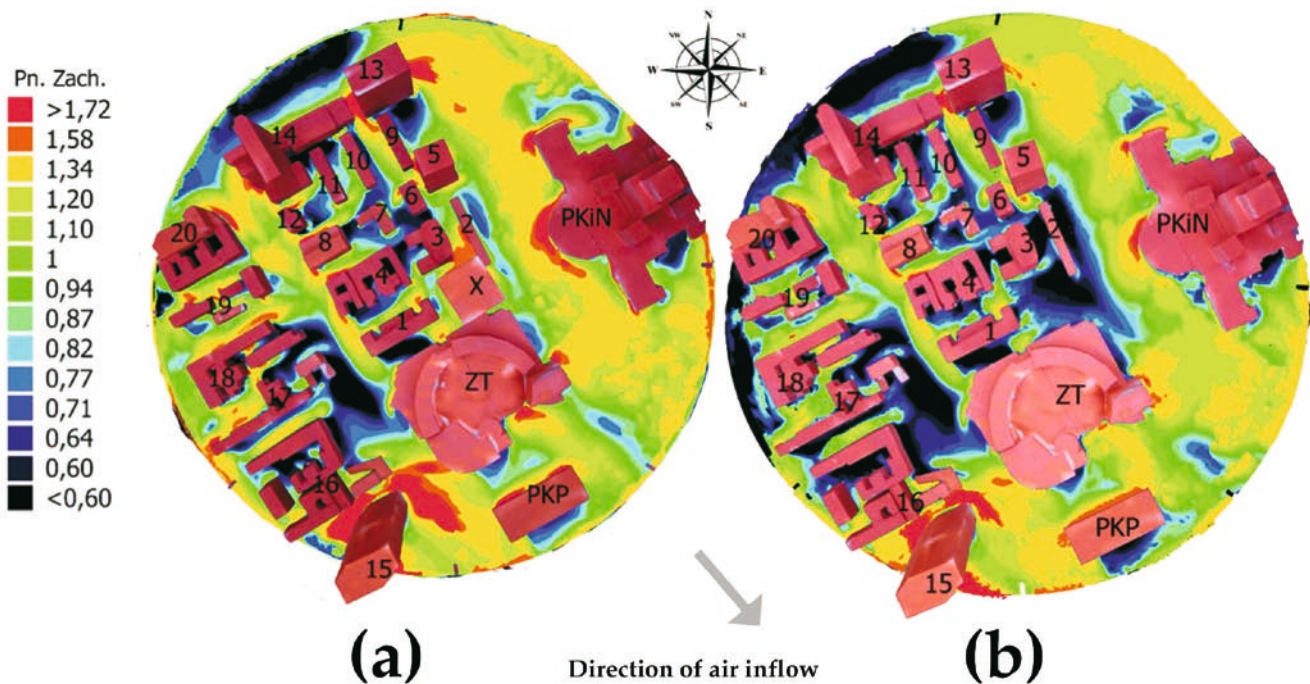


Fig. 20. Sand erosion study map for the northwest direction with (a) and without (b) a building; prepared by the authors

#### 4. DISCUSSION, SUMMARY AND CONCLUSIONS

The authors selected an urban area with a diameter of 300 m located in the center of Warsaw for the analysis. The area is characterized by dense building development of varying heights, ranging from 15 to 187 m, with a predominance of 30-metre-tall buildings.

This area is prone to the accumulation of pollutants, as the busiest communication routes in the city run through it or in its immediate vicinity. A model of this area was made in the scale of 1: 700, whereas tests were conducted in an open-circuit wind tunnel whose circular measurement space equaled 1 m. in diameter. The analysis was also based on numerical calculations, but due to the limited availability of computing power and, therefore, more time-consuming nature of numerical simulations, the geometry was simplified.

Tests in the wind tunnel were conducted for several examples of wind directions that prevail in the area under consideration. The selection was made on the basis of the analysis of the wind rose and the average velocity distribution for the city of Warsaw [(International Renewable Energy Agency, no date)].

The main objective of the study was to delineate the least ventilated zones in the studied area, i.e., those where the greatest probability of the highest concentration of both gaseous and dust pollutants occurs. For this purpose, methods applied while determining wind comfort were used (S. Reiter 2010).

The analysis described in the article concerned a specific area, whereas the methodology presented could be applied to any urbanized area in which a large concentration of various types of industrial plants and energy sources, and increased car traffic can be observed.

The analysis was performed with the use of methods applied for determining wind comfort (S. Reiter 2010), (B. Blocken, T. Stathopoulos and J.P.A.J. van Beeck 2016).

Indication of the weakest ventilation zones seems advisable, as such areas could be selected for monitoring pollution under real conditions. Currently, the use of unmanned aerial vehicles for such monitoring can be considered (T. Landolsi *et al.* 2019), (T. Villa *et al.* 2016). However, it should be remembered that in densely built-up zones, where buildings of different heights were erected, vortex structures of large dimensions appear in their vicinity. Moreover, highly accelerated airflow streams in relation to the average wind speed occur, as stems from the measurement, i.e., meteorological records for a given area. It seems, therefore, that to ensure greater safety of drone flight in densely built-up areas, it would be necessary to correlate the existing flight safety regulations for unmanned aerial vehicles for a given area with the results of wind measurements.

The research conducted in the selected quarter of the building development shows that the zones



marked in dark blue and navy blue on sand erosion maps, i.e., for which the velocity amplification coefficient is lower than 0.77, are among the least ventilated places, thus they tend to be most susceptible to pollution accumulation. When analyzing the sand erosion maps for the west and south-west wind, it can be seen that the largest air stagnation areas are visible on the leeward side of the 17-18 building complex and Galeria Złote Tarasy (the building is marked as ZT on the maps). These places where are filled with both, substantial traffic and pedestrians.

Moreover, the research considered the impact of a high-rise building, inserted into the densely built-up city tissue, on the air flow in the streets surrounding it. If they emerge among building development, high-rise buildings usually intensify the air flow and may contribute to the improvement of ventilation of the neighboring areas (T. Stathopoulos 2009), (P. Irwin, D. Scott, R. Denoon 2013). It is noteworthy that certain amount of air on the leeward side of such a building descends from higher levels to the bottom of the building, which means that the presence of a high-rise object potentially brings less polluted air to the pedestrian zone (T. Stathopoulos 2009), (Q. Xia *et al.* 2013).

Unfortunately, research on the impact of the proposed high-rise building, hypothetically located at 44 Złota Street, prompted the conclusion that for most of the analyzed planes, the presence of a conceptional tall building causes turbulence and an increase in velocity gradients. On the other hand, in the ground-level zone, the building blocks rather than intensifies the flow, i.e., it fails improve or minimally improves ventilation between buildings for certain directions of air inflow.

## LITERATURE

1. **Aristodemou E. et al. (2020)**, *Turbulent flows and pollution dispersion around tall buildings using adaptive large eddy simulation (LES)*, „Buildings” 10(10), DOI: 10.3390/BUILDINGS10070127.
2. **Blocken B. et al. (2011)**, *Application of computational fluid dynamics in building performance simulation for the outdoor environment: An overview*, „Journal of Building Performance Simulation” 4(2), pp. 157–184. DOI: 10.1080/19401493.2010.513740.
3. **Blocken B. and Carmeliet J. (2004)**, *Pedestrian wind environment around buildings: Literature review and practical examples*, „Journal of Thermal Envelope and Building Science” 28(2), pp. 107–159. DOI: 10.1177/1097196304044396.
4. **Blocken B., Stathopoulos T. and van Beeck, J.P.A.J. (2016)**, *Pedestrian-level wind conditions around buildings: Review of wind-tunnel and CFD techniques and their accuracy for wind comfort assessment*, „Building and Environment” 100, pp. 50–81. DOI: 10.1016/j.buildenv.2016.02.004.
5. **Borrego C. et al. (2006)**, *How urban structure can affect city sustainability from an air quality perspective*, „Environmental Modelling and Software” 21(4), pp. 461–467. DOI: 10.1016/j.envsoft.2004.07.009.
6. **Corrigan C. E. et al. (2008)**, *Capturing vertical profiles of aerosols and black carbon over the Indian Ocean using autonomous unmanned aerial vehicles*, „Atmospheric Chemistry and Physics”, 8(3), pp. 737–747. DOI: 10.5194/acp-8-737-2008.
7. **Dąbrowiecki P. et al. (2021)**, *Impact of Air Pollution on Lung Function among Preadolescent Children in Two Cities in Poland*, „Journal of Clinical Medicine” 10(11), p. 2375. DOI: 10.3390/jcm10112375.
8. **Duangsuwan S. and Jamjareekulgarn P. (2020)**, *Development of drone real-time air pollution monitoring for mobile smart sensing in areas with poor accessibility*, „Sensors and Materials”, 32(2), pp. 511–520. DOI: 10.18494/SAM.2020.2450.
9. **Duthinh D. and Simiu E. (2011)**, *The Use of Wind Tunnel Measurements in Building Design*, „Wind Tunnels and Experimental Fluid Dynamics Research”, (July). DOI: 10.5772/18670.
10. **En N.E. and Normy P. (2008)**, PN-EN 1991-1-4. Oddziaływania na konstrukcje. Część 1-4: Oddziaływania ogólne. Oddziaływania wiatru.
11. **Franke J. et al. (2007)**, *Best practice guideline for the CFD simulation of flows in the urban environment, COST action*. Available at: <http://cat.inist.fr/?aMod=afficheN&cpsid=23892111%5Cnhttp://scholar.google.com/scholar?hl=en&btnG=Search&q=intitle:Best+practice+guideline+for+the+CFD+simulation+of+flows+in+the+urban+environment#0>.
12. **Fronczak M. (2018)**, *Kształtowanie struktur urbanistycznych na terenach zagrożonych smogiem i zanieczyszczeniem powietrza*, „Przestrzeń, Urbanistyka, Architektura” 1, pp. 255–270. DOI: 10.4467/00000000pua.18.018.8626.
13. **Generalna Inspekcja Ochrony Środowiska** (no date), *Bieżące dane pomiarowe*, available at: <http://powietrze.gios.gov.pl/pjp/current>.
14. **Gumowski K. et al. (2015)**, *Comparative analysis of numerical and experimental studies of the airflow around the sample of urban development*, „Bulletin of the Polish Academy of Sciences: Technical Sciences” 63(3), pp. 729–737. DOI: 10.1515/bpasts-2015-0084.
15. **International Renewable Energy Agency** (no date), *Global Wind Atlas*, available at: <https://irena.masdar.ac.ae/GIS/?&tool=dtu:gwa&map=103>.
16. **Jędrzejewski M., Pocwierz M. and Zielonko-Jung K. (2017)**, *The problem of airflow around building clusters in different configurations*, „Archive of Mechanical Engineering” 64(3), pp. 401–418. DOI: 10.1515/meceng-2017-0024.
17. **Khaled M. and Dewidar K. (2010)**, *Anti Smog Architecture: a New Catalyst for Cleaner*, in: International Conference on Engineering Solutions for Sustainable Development, American University in Cairo, Cairo, doi: 10.13140/RG.2.1.4614.4242.
18. **Kiciński J. (2018)**, *Smog – Poland’s pressing problem. Anti-smog technologies in 3rd International Conference on Energy and Environmental Protection*,

- AGH University of Science and Technology, Kraków, pp. 1–7.
19. **Kleczkowski P. (2019)**, *Smog w Polsce. Przyczyny, skutki, przeciwdziałanie*, Wydawnictwo Naukowe PWN, Warszawa.
  20. **Landolsi T. et al. (2019)**, *Pollution monitoring system using position-aware drones with 802.11 Ad-Hoc networks*, 2018 IEEE Conference on Wireless Sensors, ICWiSe 2018, IEEE, pp. 40–43. DOI: 10.1109/ICWISE.2018.8633285.
  21. **Łukasz F. et al. (2019)**, *Badania modelowe dynamicznego działania na warstwę przyziemną atmosfery - wieże wentylacyjne w konfiguracji liniowej na terenie określonej chropowatości*, in *Dynamiczne przewietrzanie i redukcja smogu obszarów zurbanizowanych ze szczególnym uwzględnieniem miasta Krakowa*, Politechnika Krakowska, Kraków.
  22. **Mazurek H. and Badyda A. (2018)**, *Smog. Konsekwencje zdrowotne zanieczyszczeń powietrza*. PZWL Wydawnictwo Lekarskie, Warszawa.
  23. **Michalak A. (2020)**, *Energy Poverty in the Context of Smog As Exemplified By Poland*, GEOLINKS Conference proceedings, Book 2 Vol. 2, 2, pp. 195–204. DOI: 10.32008/geolinks2020/b2/v2/19.
  24. **O., U. S. (no date)** *Dron antysmogowy czyli System Obserwacji i Wspomagania Analizy powietrza "SOWA."*, available at: <https://usm.net.pl/produkty/1-system-obszerwacji-i-wspomagania-analizy-powietrza-sowa>.
  25. **Irwin P., Scott D., Denoon R. (2013)**, *Wind Tunnel Testing of High-Rise Buildings*, Routledge.
  26. **Rada Miasta Stołecznego Warszawy (2010)** *Uchwała NR XCIV/2749/2010 Rady Miasta Stołecznego Warszawy z dnia 9 listopada 2010 r. w sprawie miejscowego planu zagospodarowania przestrzennego w rejonie Pałacu Kultury i Nauki w Warszawie*.
  27. **Reiter S. (2008)**, *Validation Process for CFD Simulations of Wind Around Buildings*, European Built Environment CAE Conference, (November), pp. 1–18, available at: <http://orbi.ulg.ac.be/handle/2268/20400>.
  28. **Reiter S. (2010)**, *Assessing wind comfort in urban planning*, „Environment and Planning B: Planning and Design”, 37(5), pp. 857–873. doi: 10.1068/b35154.
  29. **Sanz-Rodrigo J., van-Beeck J.P.A.J., Dezsö-Weidinger G. (2007)**, *Wind tunnel simulation of the wind conditions inside bidimensional forest clear-cuts. Application to wind turbine siting*, „Journal of Wind Engineering and Industrial Aerodynamics” 95(7), pp. 609–634. DOI: doi.org/10.1016/j.jweia.2007.01.001.
  30. **Schwartz J., Laden F. and Zanobetti A. (2002)**, *The Concentration – Response Relation between PM<sub>2.5</sub> and Daily Deaths*, „Environmental Health Perspectives”, 110(10), pp. 1025–1029.
  31. **Stanaszek-Tomal, E. (2021)**, *Anti-Smog Building and Civil Engineering Structures*, „Processes”, 9 (8), p. 1446. DOI: 10.3390/pr9081446.
  32. **Stathopoulos T. (2009)**, *Wind and comfort*, in 5th European and African Conference on Wind Engineering, EACWE 5, Proceedings.
  33. **Stathopoulos T. (2011)**, *Introduction to environmental aerodynamics*, in „CISM International Centre for Mechanical Sciences, Courses and Lectures”, Concordia University, Montreal, pp. 3–30. doi: 10.1007/978-3-7091-0953-3\_1.
  34. **Szymocha S. and Osuchowski J. (2019)**, *Pomiary przy pomocy bezzałogowych statków powietrznych. Diagnostyka linii wysokiego napięcia*, Fundacja na Rzecz Czystej Energii, Poznań.
  35. **Tominaga, Y. et al. (2008)**, *AIJ guidelines for practical applications of CFD to pedestrian wind environment around buildings*, „Journal of Wind Engineering and Industrial Aerodynamics”, 96(10–11), pp. 1749–1761. DOI: 10.1016/j.jweia.2008.02.058.
  36. **Villa, T. et al. (2016)**, *An overview of small unmanned aerial vehicles for air quality measurements: Present applications and future perspectives*, „Sensors”, 16(7), pp. 12–20. doi: 10.3390/s16071072.
  37. **Xia, Q. et al. (2013)**, *Effects of building lift-up design on pedestrian wind environment*, in Proceedings of the 8th Asia-Pacific Conference on Wind Engineering, APCWE 2013, pp. 993–1002. DOI: 10.3850/978-981-07-8012-8\_128.